

Regular and Static Sector-Based Cell Switch-Off Patterns

Tamer Beitelmal, Sebastian S. Szyszkowicz, and Halim Yanikomeroglu

Department of Systems and Computer Engineering, Carleton University, Canada
{tamer, sz, halim}@sce.carleton.ca

Abstract—Energy saving in cellular networks can be achieved by implementing the cell switch-off (CSO) approach in periods of light traffic. Regular static CSO (CSO patterns) is a type of CSO where the set of active cells is predetermined such that they are located on a regular grid. It is known that regular cell layouts generally provide the best coverage and downlink SINR. Furthermore, CSO patterns assure that interfering cells are as far away as possible and help in modeling interference accurately. Existing literature on CSO patterns focuses only on site-level CSO (switching off entire BSs); however, significant gains can sometimes be obtained from sector-level CSO patterns (switching off individual sectors).

This paper is the first to introduce and investigate sector-based regular CSO patterns by providing illustrative examples. We compare the performances of different CSO patterns in terms of the number of supported users. Also, we analytically compare site-based versus sector-based CSO patterns in terms of power saving. Our results show that patterns with only one of the three sectors active (each with the same orientation) can support the most users per sector, due to a favourable interference situation.

Index Terms—Green Communications, LTE, Cell Switch-Off (CSO), Regular Static CSO, Sector-Based CSO Patterns.

I. INTRODUCTION

The number of base stations (BSs) has been increasing rapidly to serve the growing demand for high data rates, and sometimes over-provisioning to cope with peak traffic. This leads to many BSs being underutilized in periods of light traffic. The fact that, in cellular networks, most of the power is consumed by BSs regardless of their load motivates the cell switch-off (CSO) approach. CSO aims at switching off some unnecessary BSs without sacrificing the quality of service for user equipments (UEs) or affecting the coverage area (see survey papers [1, 2] for details).

When a cell is switched off, its UEs need to be reassigned to neighbouring cells, perhaps less advantageous in terms of SINR. This reassignment of UEs requires proper interference characterization; one accurate way to model interference is by predetermining the set of active cells, i.e., the cells that actually generate the interference in the system. This is sometimes referred to as offline or static CSO [1, 2]. Different sets of active cells are predetermined offline, and the operator selects the appropriate set to

accommodate the current traffic density [3]. Offline CSO is usually applicable for longer switching durations (in the order of hours) and is often based on historical load distribution. Therefore, the interference can be modeled appropriately (in statistical terms) by including only the predetermined set of active cells [4].¹

Regular static CSO (*CSO patterns*) is a special case of static CSO, where active BSs are predetermined such that their locations form a periodic (regular) pattern [2]. A *pattern* is the configuration of active BSs, which is repeated in a spatially periodic manner. CSO patterns are already under consideration by several research groups [4–11]. The effect of different CSO patterns on the outage probability is investigated in [4, 6], while the effect on the blocking probability is studied in [8, 10]. Authors in [11] introduce a set of CSO patterns and propose a scheduler to jointly ensure full coverage for both downlink and uplink. Regular CSO patterns resemble the intuitive well-known frequency reuse patterns. It was shown that, for the same number of BSs, the best SINR distribution can be achieved when the BSs are located on a regular grid [12], which guarantees that interfering cells are as far away as possible, and reduces the coverage holes. Also, it is more energy-efficient for UEs in the uplink when there is always a nearby cell [13, 14].

Contributions: Previous literature on regular CSO patterns only studies switching off entire BSs (*site-level*), however, additional gain may be obtained from switching off individual sectors within each BS (*sector-level*). To the best of our knowledge, this is the first paper to introduce sector-based CSO patterns and compare their performance in terms of number of supported UEs. We also analytically compare the site-level versus sector-level power saving.

This paper is organized as follows: Section II discusses the newly-introduced sector-based CSO and studies their power consumption. Section III describes the simulation setup, while Section IV provides a case study, comparing the performance of some CSO patterns. Section V concludes the paper.

¹Static CSO can be seen as a cell planning problem, but with a constrained set of BS locations. While in cell planning, the BS placement is based on a wider set of possible locations, in CSO, the locations are restricted to the actual sites of BSs, from which a subset is chosen to be active.

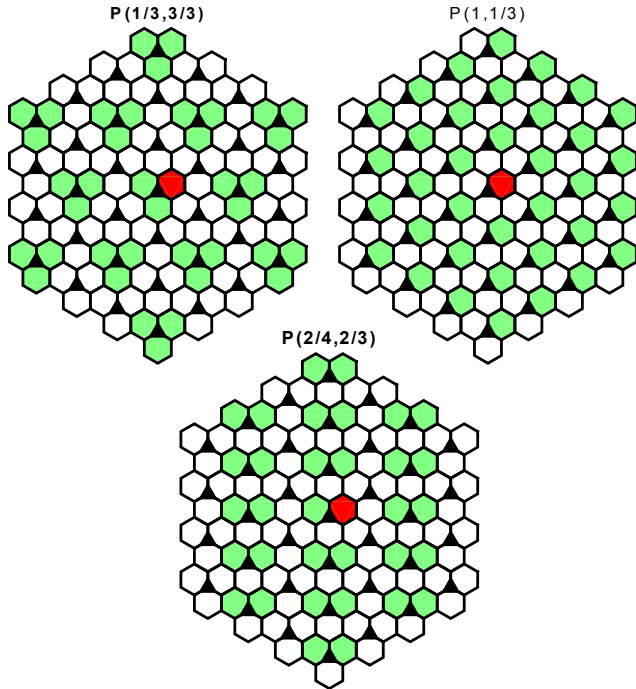


Figure 1. Different patterns with $\rho = 1/3$ active sectors.

II. METHODOLOGY

A. Sector-Based CSO Patterns

The patterns are denoted as $P(n/m, k/3)$, where the first term inside parenthesis corresponds to the site-level pattern (the proportion n/m of active BSs), and the second term corresponds to the sector-level pattern (the number k of active sectors per BS). The proportion of active sectors is $\rho = |P(n/m, k/3)| = \frac{nk}{3m} \in [0, 1]$. Therefore, the pattern for which all BSs and all sectors are active (i.e., without CSO) is referred to as $P(1, 3/3)$.

In order to further illustrate this idea, we focus on four interesting examples, each having CSO patterns with the same proportion of active sectors, but with different sector configuration. These patterns are illustrated in Figs. 1–4, where black triangles represent BS (site) locations, and each site has three sectors. The UE is connected to sector 1 (the red hexagon). Green hexagons are active sectors, which cause interference to the UE, while white hexagons are switched-off sectors.

1) *One third of the sectors are active:* This example illustrates three patterns where one third of the sectors are active (i.e., $\rho = \frac{1}{3}$), namely: $P(1, 1/3)$ (where all BSs are active with one out of three active sectors), $P(1/3, 3/3)$ (where one out of three BSs is active with all sectors are active), and $P(2/4, 2/3)$ (where two out of four BSs are active, each with two out of three active sectors).

2) *One fourth of the sectors are active:* This example illustrates two patterns where one fourth of the sectors are active (i.e., $\rho = \frac{1}{4}$), namely: $P(1/4, 3/3)$ and $P(3/4, 1/3)$.

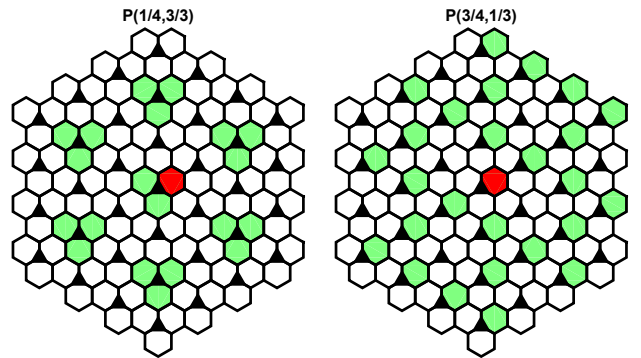


Figure 2. Two patterns with $\rho = 1/4$ active sectors.

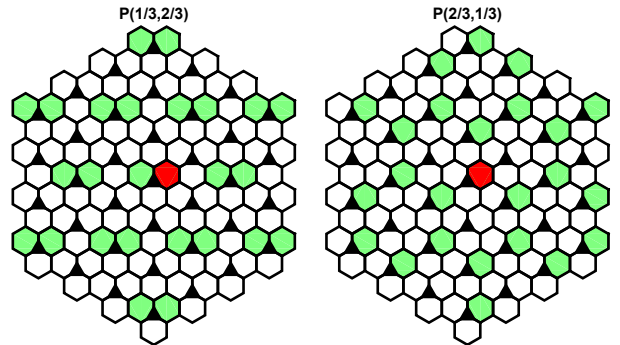


Figure 3. Two patterns with $\rho = 2/9$ active sectors.

3) *Two ninths of the sectors are active:* This example illustrates two patterns where two ninths of the sectors are active (i.e., $\rho = \frac{2}{9}$), namely: $P(1/3, 2/3)$ and $P(2/3, 1/3)$.

4) *One sixth of the sectors are active:* This example illustrates two patterns where one sixth of the sectors are active (i.e., $\rho = \frac{1}{6}$), namely: $P(1/4, 2/3)$ and $P(2/4, 1/3)$.

B. Performance Metrics

The average number of supported UEs is used as the metric to compare the performance of different CSO patterns. UE i is connected to the sector that provides it with

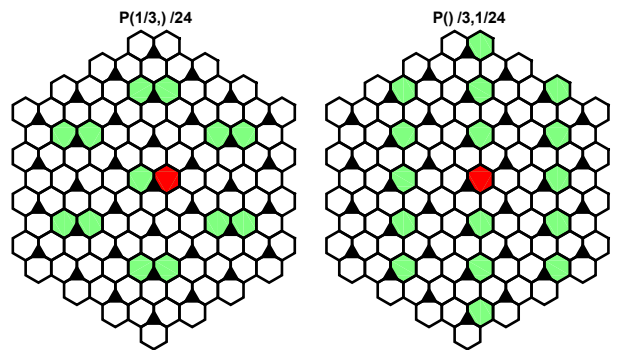


Figure 4. Two patterns with $\rho = 1/6$ active sectors.

the best downlink SINR γ_i . Hence the downlink spectral efficiency η_i of UE $_i$ is found to be

$$\eta_i = \log_2(1 + \gamma_i) \text{ [bps/Hz]}. \quad (1)$$

Because the patterns are periodic in space, sector 1 is representative of the whole network. Among the UEs that select to connect to sector 1, some of them might have a very weak SINR ($< \gamma_{\min}$), and the UE cannot receive any useful signal, and is in outage. Other UEs have very high SINR ($> \gamma_{\max}$), higher than what the current constellations can utilize; therefore, these high SINRs are truncated.²

UEs are admitted to the network on a first-come first-served basis regardless of their bandwidth demand b_i :

$$b_i = \frac{R}{\eta_i}, \quad (2)$$

which depends on η_i , and the UE's downlink rate requirement R .

UEs are admitted one-by-one, their bandwidth requirement are added up until the next UE exceeds the bandwidth W . Thus the capacity constraint is

$$\sum_{i=1}^N b_i \leq W. \quad (3)$$

The average number of UEs per active sector is then close to $W/\mathbb{E}\{b\}$, which is

$$\mathbb{E}\{N\} \cong \frac{W}{R \mathbb{E}\left\{\frac{1}{\eta}\right\}}. \quad (4)$$

The average number of UEs per system sector is $\rho \mathbb{E}\{N\}$. The total number of UEs supported by the network is found by multiplying $\rho \mathbb{E}\{N\}$ by the total number of sectors in the network.

C. Power Saving in Sector Switch-Off

In CSO literature, the amount of energy saving is assumed to be proportional to the proportion of switched-off sectors ($1 - \rho$). Although this is a valid assumption, especially since the power consumption of a BS is highly independent of its load [3, 16, 17]; it is worth investigating the power saving ratio between site switch-off and sector switch-off. In a typical LTE network, each BS has three sectors; however, switching off one sector per BS does not necessarily result in one third of energy saving. This is because there is common hardware that is shared among the three sectors at each site, such as cooling and baseband processing equipment. A site with all three sectors active consumes a total power of

$$P_{\text{site}} = P_C + 3P_S, \quad (5)$$

where P_C is the common power consumed at a site, and P_S is the additional power consumed per individual sector.

² For LTE networks, typical values for γ_{\min} and γ_{\max} are -7 dB and 18 dB, respectively [15].

We now compare two patterns which have the same proportion of active sectors $\rho = \frac{n}{3m}$. For pattern P($n/m, 1/3$), the average power consumption per system site

$$P_{\text{pattern},1} = \frac{n}{m}(P_C + 1P_S), \quad (6)$$

and for pattern P($n/3m, 3/3$), we have

$$P_{\text{pattern},2} = \frac{n}{3m}(P_C + 3P_S). \quad (7)$$

We compare the consumed power per UE, and find the breakpoint using

$$\frac{P_{\text{pattern},1}}{\mathbb{E}\{N_1\}} = \frac{P_{\text{pattern},2}}{\mathbb{E}\{N_2\}}, \quad (8)$$

$$\Rightarrow \frac{\frac{n}{m}(P_C + 1P_S)}{\frac{n}{3m}(P_C + 3P_S)} = \frac{\mathbb{E}\{N_1\}}{\mathbb{E}\{N_2\}}. \quad (9)$$

After some simplifications we obtain

$$\frac{(1 + \alpha)}{(1 + \frac{\alpha}{3})} = \frac{1}{\delta}, \quad (10)$$

where $\delta = \mathbb{E}\{N_2\}/\mathbb{E}\{N_1\}$ and $\alpha = P_C/P_S$.³

Finally, we can find the breakpoint as

$$\alpha^* = \frac{1 - \delta}{\delta - \frac{1}{3}}. \quad (11)$$

If $\alpha < \alpha^*$, then the site-level pattern P($n/3m, 3/3$) is more efficient; otherwise, the pattern P($n/m, 1/3$) with 1/3 active sectors is preferred. Similar calculations can be done for the case of 2/3 active sectors; however, we will find in the next section that those patterns are not very advantageous in terms of energy efficiency, regardless of α .

III. SIMULATION

In this paper, we consider the downlink performance for a cellular network with hexagonal layout. The simulation results are obtained using the Urban Macro-cell (UMA) scenario, according to the evaluation guidelines of [18]. The simulation parameters are listed in Table I.

The patterns are assumed to be periodic, i.e., they expand to infinity. We consider enough interfering BSs to obtain accurate SINR values for UEs connected to sector 1. For each CSO pattern, we simulate many UEs to estimate the average number of UEs that can be served by sector 1.

Fig. 5 compares the performance of different CSO patterns. The x-axis is the average number of UEs per system sector. The y-axis is proportional to the total energy saving (when $\alpha = 0$). The system energy consumption is computed from both the y-axis value and the marker type; different markers indicate the number of active sectors per BS site. The reference line gives locations where the performance of the network is scaled proportionally with respect to the fully active network P(1, 3/3). The trend is that patterns with all sectors active fall close to the reference line, as do patterns with two active sectors per

³The value of α would be known by the network operator.

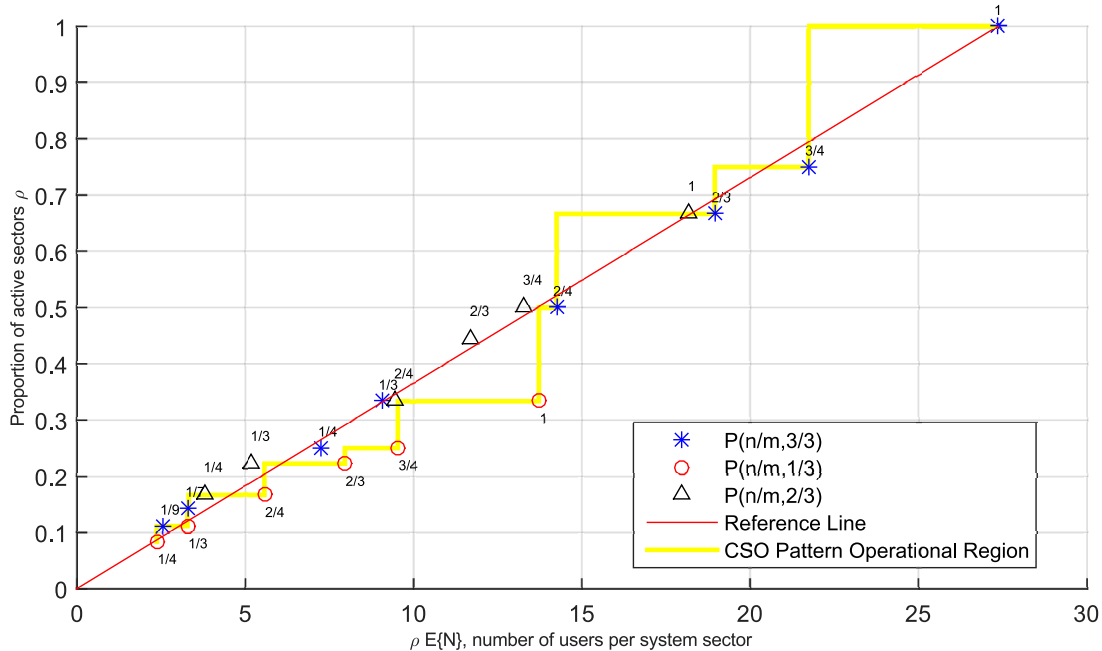


Figure 5. Performance comparison of different CSO patterns. The x-axis is the average number of UEs supported per system sector when $W/R = 20$. The y-axis is proportional to the total energy saving. Different marker types indicate the number of active sectors per BS. The reference line gives locations where the performance of the network is scaled proportionally with respect to the fully active network $P(1, 3/3)$. The operational region curve follows the best performing pattern for any given ρ . Patterns with $\rho > 1/6$ have outage probability of $< 2\%$, while the remaining patterns have outage probability between 2% and 9%.

Table I
SIMULATION PARAMETERS FOR URBAN MACROCELL (UMA)
SCENARIOS

Parameter	Assumption
Cellular layout	hexagonal
Sectorization	three 120° sectors
Antenna pattern	[18, Sec. 8.5]
System bandwidth	10 MHz
UE required rate	500 kbps
Inter-site distance	500 m
BS antenna height	25 m
Cell transmitted power	46 dBm
Carrier frequency (f_c)	2.0 GHz
UE distribution	independent and uniform
Probability of indoor UEs	0
UE noise figure	5 dB
BS noise figure	7 dB
Thermal noise	-174 dBm/Hz
Shadowing spread (LOS)	4 dB
Shadowing spread (NLOS)	6 dB
SINR range	[-7, 18] dB
Traffic type	full queue

BS. Interestingly, patterns with one active sector per BS fall to the right of the line (perform better). Notably, consider the case of $\rho = 1/3$: the number of active sectors is reduced to one third; however, the average number of UEs that can be supported by pattern $P(1, 1/3)$ is only reduced to half the full capacity of $P(1, 3/3)$. The yellow staircase curve shows the operational region based on the

best performing pattern for any given ρ ; this curve can be used by operators to select the best pattern to support a given user density demand.

IV. CASE STUDY

In this section, we further investigate CSO patterns with $\rho = 1/3$, shown in Fig. 1.

A. SINR Distribution

Fig. 6 shows the effect of applying different CSO patterns on the resulting cumulative distribution function (CDF) of the SINR for UEs connected to sector 1. Very high SINR values were obtained from pattern $P(1, 1/3)$, with only one active sector per BS. This improvement is due to the reduction in the number of nearby interferers as all active sectors are pointing in the same direction. However, higher SINR values are truncated at 18 dB [15]; these higher values might be of interest in future systems that allow for higher constellations.

B. Number of Users per Active Sector

The distribution of the number of UEs supported by an active sector is shown in Fig. 7 for each pattern: Pattern $P(1, 1/3)$ can support the most UEs (41) per active sector on average, and about 32 UEs 95% of the time. The number of UEs closely follows a Gaussian distribution.

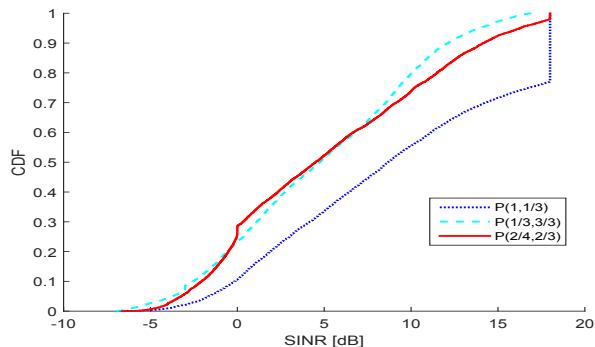


Figure 6. CDFs of SINR for patterns in Fig. 1 (with $\rho = 1/3$).

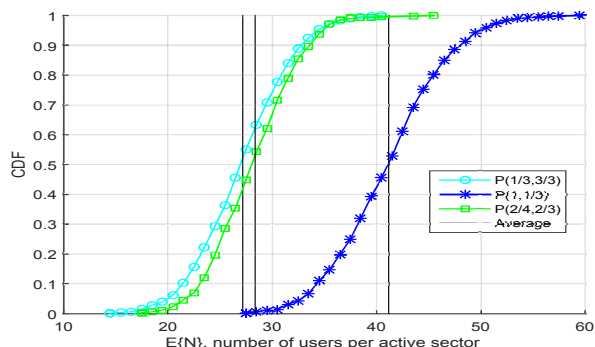


Figure 7. CDFs of the number of UEs per active sector for patterns in Fig. 1 (with $\rho = 1/3$), when $W/R = 20$. Each CDF closely follows a Gaussian distribution.

C. Energy Efficiency Aspects

Based on the calculations in Section II-C, we can find the breakpoint that indicates which pattern is better in terms of energy efficiency per UE. While the patterns with 2/3 active sectors are never very advantageous, the pattern $P(1, 1/3)$ is advantageous over pattern $P(1/3, 3/3)$ as long as $P_S/P_C > \alpha = 0.9524$, as found from (11).

V. CONCLUSION

While regular CSO patterns have been studied in the literature, this paper is the first to investigate regular sector-based CSO patterns, where switching off individual sectors per BS is allowed. We compared the performance of these patterns in terms of the number of users a pattern can support. Notably, patterns with one active sector per active BS (the same sector in each BS) perform best due to a favourable interference situation. In particular, when all BSs are on with only one active sector each, the system can support half the number of users of the fully active network, and even more if higher SINR values are supported in future networks.

ACKNOWLEDGMENT

The authors would like to thank David González G., from Aalto University-Finland, for his valuable discussions. This work is funded by TELUS, Canada, and by

the Ministry of Higher Education and Scientific Research (MOHESR), Libya, through the Libyan-North American Scholarship Program.

REFERENCES

- [1] L. Budzisz, F. Ganji, G. Rizzo, M. Marsan, M. Meo, Y. Zhang, G. Koutitas, L. Tassiulas, S. Lambert, B. Lannoo, M. Pickavet, A. Conte, I. Haratcherev, and A. Wolisz, "Dynamic resource provisioning for energy efficiency in wireless access networks: A survey and an outlook," *IEEE Commun. Surveys Tuts.*, vol. 16, no. 4, pp. 2259–2285, 4th quarter 2014.
- [2] K. C. Tun and K. Kunavut, "An overview of cell zooming algorithms and power saving capabilities in wireless networks," *KMUTNB: International Journal of Applied Science and Technology*, vol. 7, no. 3, pp. 1–13, July 2014.
- [3] D. González, H. Yanikomeroglu, M. Garcia-Lozano, and S. Ruiz Boque, "A novel multiobjective framework for cell switch-off in dense cellular networks," in *IEEE International Conference on Communications (ICC)*, June 2014, pp. 2641–2647.
- [4] S. Kokkinogenis and G. Koutitas, "Dynamic and static base station management schemes for cellular networks," in *IEEE Global Communications Conference (GLOBECOM)*, Dec. 2012, pp. 1–6.
- [5] "Telecommunication management; study on energy savings management (ESM)," 3rd Generation Partnership Project (3GPP), TR 32.826, Apr. 2010.
- [6] F. Han, Z. Safar, W. Lin, Y. Chen, and K. Liu, "Energy-efficient cellular network operation via base station cooperation," in *IEEE International Conference on Communications (ICC)*, June 2012, pp. 4374–4378.
- [7] M. Marsan, L. Chiaraviglio, D. Ciullo, and M. Meo, "Optimal energy savings in cellular access networks," in *IEEE International Conference on Communications Workshops (ICC)*, June 2009, pp. 1–5.
- [8] X. Weng, D. Cao, and Z. Niu, "Energy-efficient cellular network planning under insufficient cell zooming," in *IEEE Vehicular Technology Conference (VTC Spring)*, May 2011, pp. 1–5.
- [9] L. B. Le, "QoS-aware BS switching and cell zooming design for OFDMA green cellular networks," in *IEEE Global Communications Conference (GLOBECOM)*, Dec. 2012, pp. 1544–1549.
- [10] L. Chiaraviglio, D. Ciullo, M. Meo, and M. A. Marsan, "Energy-efficient management of UMTS access networks," in *Proc. IEEE International Teletraffic Congress (ITC)*, Sept. 2009, pp. 1–8.
- [11] A. Kumar and C. Rosenberg, "Energy and throughput trade-offs in cellular networks using base station switching," *IEEE Trans. Mobile Comput.*, vol. 15, no. 2, pp. 364–376, Feb. 2016.
- [12] A. Guo and M. Haenggi, "Spatial stochastic models and metrics for the structure of base stations in cellular networks," *IEEE Trans. Wireless Commun.*, vol. 12, no. 11, pp. 5800–5812, Nov. 2013.
- [13] L. Suárez, L. Nuaymi, and J.-M. Bonnin, "Energy-efficient BS switching-off and cell topology management for macro/femto environments," *Computer Networks*, vol. 78, pp. 182–201, Nov. 2014.
- [14] I. Aydin, H. Yanikomeroglu, and U. Aygolu, "User-aware cell switch-off algorithms," in *IEEE International Wireless Communications & Mobile Computing Conference (IWCMC)*, Aug. 2015, pp. 1236–1241.
- [15] "Calibration for IMT-Advanced Evaluations," CELTIC/CP5-026 Project WINNER+, Munich, Germany, Tech. Rep., May 2010.
- [16] T. Beitelmal and H. Yanikomeroglu, "A set cover based algorithm for cell switch-off with different cell sorting criteria," in *IEEE International Conference on Communications (ICC)-Workshops*, June 2014, pp. 641–646.
- [17] F. Alaca, A. Bin Sediq, and H. Yanikomeroglu, "A genetic algorithm based cell switch-off scheme for energy saving in dense cell deployments," in *IEEE Global Communications Conference Workshops (GLOBECOM)*, Dec. 2012, pp. 63–68.
- [18] ITU-R, "Report ITU-R M.2135-1; guidelines for evaluation of radio interface technologies for IMT-Advanced," 2009.